

Determination of exciton transition energy and bowing parameter of AlGa_N alloys in AlGa_N/Ga_N heterostructure by means of reflectance measurement

著者 (英)	H. Jiang, G. Y. Zhao, H. Ishikawa, Takashi Egawa, Takashi Jimbo, Masayoshi Umeno
journal or publication title	JOURNAL OF APPLIED PHYSICS
volume	89
number	2
page range	1046-1052
year	2001-01-15
URL	http://id.nii.ac.jp/1476/00004906/

doi: 10.1063/1.1334923(<http://dx.doi.org/10.1063/1.1334923>)

Determination of exciton transition energy and bowing parameter of AlGaN alloys in AlGaN/GaN heterostructure by means of reflectance measurement

H. Jiang^{a)}

Department of Environmental Technology and Urban Planning, Nagoya Institute of Technology, Gokiso-cho, Showa-ku, Nagoya 466-8555, Japan

G. Y. Zhao, H. Ishikawa, and T. Egawa

Research Center for Micro-Structure Devices, Nagoya Institute of Technology, Gokiso-cho, Showa-ku, Nagoya 466-8555, Japan

T. Jimbo

Department of Environmental Technology and Urban Planning, Nagoya Institute of Technology, Gokiso-cho, Showa-ku, Nagoya 466-8555, Japan

M. Umeno

Research Center for Micro-Structure Devices, Nagoya Institute of Technology, Gokiso-cho, Showa-ku, Nagoya 466-8555, Japan

(Received 28 August 2000; accepted for publication 30 October 2000)

The normal-incidence reflectance measurement was employed to obtain the free exciton transition energy (E_{FX}) of AlGaN alloys in $Al_xGa_{1-x}N/GaN/sapphire$ heterostructure grown by metalorganic chemical vapor deposition. It was found that the thickness variation of the AlGaN layer may cause a noticeable change in the line shape of reflectance spectrum and impede the identification of the desired excitonic position. By using a reflection model of two absorbing layers with a transparent substrate, the experimental reflectance spectra were theoretically simulated and utilized to explain the reflection mechanism in $Al_xGa_{1-x}N/GaN$ heterostructures. On the basis of the above analysis, the feasibility of the reflectance measurement for such heterostructures is confirmed. At room temperature, the E_{FX} s obtained from the fitting showed an excellent agreement with the corresponding peak energies in the photoluminescence spectra. Furthermore, at the optical energy position about 100 meV above the E_{FX} , the spectral feature of exciton-LO phonon interaction was observed in the reflectance spectrum record for low Al composition ($x \leq 0.16$). Using the Al mole fraction derived from x-ray diffraction measurement, the bowing parameter of the epitaxial AlGaN layer was determined. In the range of $0 \leq x < 0.3$, the resulting bowing parameter shows a downward value of 0.53 eV. © 2001 American Institute of Physics. [DOI: 10.1063/1.1334923]

I. INTRODUCTION

GaN and its heterostructure with AlGaN have attracted much attention to fabricate high power/high speed hetero-junction field-effect transistors¹ as well as near UV laser diodes² and vision-blind UV detectors.³ In such device applications, a crucial property of the AlGaN alloys is the composition dependence of the band gap energy (E_g), which is described by a linear behavior of Al mole fraction (x) and a nonlinear deviation of bowing parameter (b). Up to now, a number of investigations have been done on the determination of the two parameters x and b .⁴ Although the composition of AlGaN alloys obtained by chemical evaluation methods, such as electron probe microanalysis (EPMA) or Rutherford-backscattering spectrometry (RBS), etc., is considered more accurate than that extracted from the measurement of x-ray diffraction (XRD), it was suggested recently that with taking account of the in-plane biaxial strain effect on both lattice parameters, a and c , the XRD method is also

possible to generate precise Al content and, furthermore, provides information about the microstructure of epitaxial layers.⁵ On the other hand, for the bowing parameter, because the investigations were performed on samples in different structures, growth methods, and growth conditions, it is difficult to present a universal constant. In fact, there has been a relatively large variance in the values of bowing parameter reported so far.⁴ Therefore in practical meaning, providing a simple and effective method seems more useful than trying to give a unified value of bowing parameter.

Reflectance measurement as a powerful method has been used in many works to yield the knowledge of optical constants and excitonic resonance structure of III-V column semiconductor materials.⁶⁻⁸ The three characteristic excitons (A , B , and C) of the wurtzite crystal structure GaN and AlGaN are usually used to deduce the band gap energy (E_g). For GaN, the large exciton binding energy permits its excitons to exist even at room temperature. It is predictable that for $Al_xGa_{1-x}N$ also, the excitons will exist and strongly influence the room temperature band structure, specially in low Al composition region. On the other hand, reflectance mea-

^{a)}Electronic mail: jianghao_jp@yahoo.com

surement is, if possible, obviously convenient in determining the E_g of AlGaN alloys, compared with other optical spectroscopic methods, such as photoluminescence (PL), cathodoluminescence (CL), and optical absorption (OA) measurements. The recent study of Ochalski *et al.* has employed reflectance and photorelectance (PR) spectra to determine the E_{FX} of AlGaN, but without any discussion on reflectance measurement.⁹ More recently, Yu *et al.* have confirmed the feasibility of this measurement in estimating the E_g of AlGaN alloys in AlGaN/GaN heterostructures, but with a difference of 3% (above 100 meV) compared with PL measurement.¹⁰ In the experiment, however, we found that the thickness variation of the AlGaN layer may change the line shape of reflectance spectrum and create uncertainty in determining the location of excitonic energy. It was shown that this uncertainty may be the reason for the large discrepancy between the reflectance and PL measurements. Hence the application of this method remains to be elucidated in model analysis and accuracy modification. For such purposes, a reflection model of two absorbing layers with a transparent substrate was used to perform a detailed discussion on the experimental data. Based on this discussion, the E_{FXS} of AlGaN obtained from a fitting procedure were found in an excellent agreement with that from PL measurement. Combining the results of the reflectance and XRD measurements, we obtained a downward bowing parameter $b=0.53$ eV in the excitonic transition band gap of AlGaN epilayer.

II. EXPERIMENTAL PROCEDURE

The samples in this study were grown on sapphire (0001) substrate by the horizontal atmospheric pressure metal-organic chemical-vapor deposition (MOCVD) method. Trimethylgallium (TMGa), trimethylaluminum (TMAI), and ammonia (NH₃) were used as source materials for Ga, Al, and N. All the epitaxial layers were nominally undoped. The sapphire substrate was first heated at 1100 °C for 10 min in a stream of hydrogen for cleaning. Then the temperature was lowered to 500 °C to grow a 30 nm GaN buffer layer. Subsequently, the temperature was elevated to 1080 °C, at which a 1.5- μ m-thick GaN layer and a AlGaN layer with a thickness between 30 and 200 nm was grown. The heterostructure is illustrated in Fig. 1. Reflection spectrum was measured in air for light normally incident to the surface of the sample with a 0.1 nm spectral resolution. A tungsten lamp was used as the light source. The peaks in reflectance spectra have also been confirmed by He–Cd laser source (325 nm) PL measurement for low Al composition samples. XRD measurement used a rotating anode Rigaku RINT2000 diffractometer, with Cu $K\alpha_1/K\alpha_2$ doublet ($K\alpha_1=0.1540562$ nm). The scan step was 0.002°. All measurements were carried out at room temperature.

III. RESULTS AND DISCUSSION

A. Composition of the AlGaN layer

For wurtzite structure Al_xGa_{1-x}N crystal, the lattice parameter of principle crystal axis c can be obtained from XRD measurement in the symmetric (0006) reflections of $2\theta-\theta$ mode by using the Bond method. The value for c is often

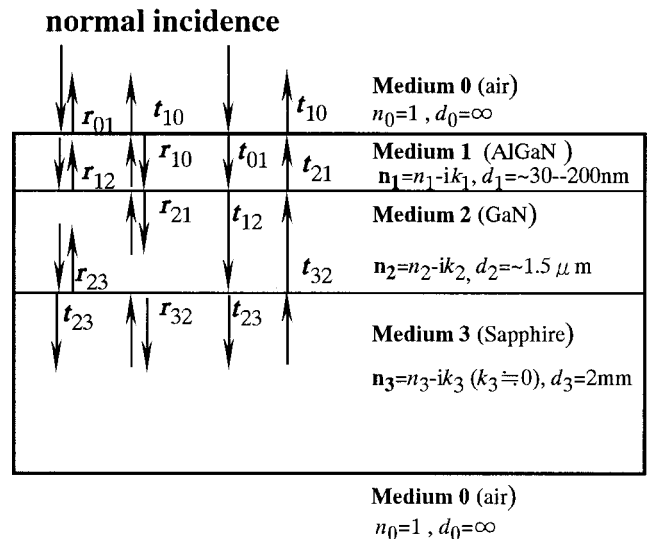


FIG. 1. Schematic diagram of the AlGaN/GaN/sapphire heterostructure and the reflection and transmission of the normal-incidence light in this multi-layered system.

used to calculate the mole fraction (x) assuming the validity of Vegard’s law. Principally, the relaxed lattice parameters a_0 and c_0 from the binaries AlN and GaN, $a_0(x)$ and $c_0(x)$ of stress-free ternary Al_xGa_{1-x}N films should be related to mole fraction (x) by the linear expression

$$c_0(x) = c_0^{\text{GaN}}(1-x) + c_0^{\text{AlN}}x, \tag{1a}$$

$$a_0(x) = a_0^{\text{GaN}}(1-x) + a_0^{\text{AlN}}x, \tag{1b}$$

where the fully relaxed lattice constants a_0 and c_0 are taken to be 3.1892 and 5.1850 Å for GaN,¹¹ and 3.1114 and 4.9792 Å for AlN,¹² respectively, values which are now widely accepted. However, in most cases, the lattice parameters are changed by lattice mismatch, thermal expansion change, point defects, and size effect, etc.¹³ In view of these changes, the actual lattice parameters a and c could be, under a crucial assumption that in-plane biaxial strain is dominant in the AlGaN layer, related to the fully relaxed ones by strain ratio,

$$\varepsilon_c/\varepsilon_a = \frac{(c-c_0)}{c_0} \bigg/ \frac{(a-a_0)}{a_0} = -2 \frac{C_{13}}{C_{33}}, \tag{2}$$

where C is the elastic stiffness constants of the AlGaN epitaxial layer. Considering that the elastic properties of ternary varies linearly with the composition of arbitrary binary compounds, AlN and GaN, the values $C_{13}=114$ and $C_{33}=381$ GPa ($\varepsilon_c/\varepsilon_a = -0.60$) for GaN (Ref. 14) and $C_{13}=120$ and $C_{33}=395$ GPa ($\varepsilon_c/\varepsilon_a = -0.61$) for AlN (Ref. 15) were used to set the value of strain ratio of AlGaN as -0.60 here, which is also identical to that used by Akasaki *et al.* in Ref. 16.

The mole fraction x of the alloys can then be calculated by solving Eqs. (1) and (2). Because the AlGaN films are so thin in this experiment and all samples show relative high 2DEG mobility, they can be considered as perfectly strained by GaN layers, and then we can assume that $a_0(x) = a_0^{\text{GaN}}$ here. The composition values therefore obtained from the measured lattice constants are shown in the next section.

B. Interpretation of reflectance spectra

In Fig. 1, the AlGaIn/GaN/sapphire multilayered structure is drawn schematically. Assuming that the thickness of sapphire substrate is infinite and the roughness of the top most epilayer is negligible, at normal incident, the power reflectance of this structure which takes the multiple reflection into consideration can be written as

$$R = |r|^2 = \left| r_{02} + \frac{t_{02}t_{20}r_{23} \exp(-2\alpha_2 d_2) \exp(-i\delta_2)}{1 - r_{23}r_{20} \exp(-2\alpha_2 d_2) \exp(-i\delta_2)} \right|^2, \quad (3)$$

where

$$r_{02} = \frac{r_{01} + r_{12} \exp(-2\alpha_1 d_1) \exp(-j\delta_1)}{1 - r_{10}r_{12} \exp(-2\alpha_1 d_1) \exp(-j\delta_1)}, \quad (3a)$$

$$r_{20} = \frac{r_{21} + r_{10} \exp(-2\alpha_1 d_1) \exp(-j\delta_1)}{1 - r_{10}r_{12} \exp(-2\alpha_1 d_1) \exp(-j\delta_1)}, \quad (3b)$$

$$t_{02} = \frac{t_{01}t_{12} \exp(-\alpha_1 d_1) \exp(-j\delta_1/2)}{1 - r_{10}r_{12} \exp(-2\alpha_1 d_1) \exp(-j\delta_1)}, \quad (3c)$$

$$t_{20} = \frac{t_{21}t_{10} \exp(-\alpha_1 d_1) \exp(-j\delta_1/2)}{1 - r_{10}r_{12} \exp(-2\alpha_1 d_1) \exp(-j\delta_1)}, \quad (3d)$$

and

$$r_{ij} = \left| \frac{(n_i - n_j)^2 + (\kappa_i - \kappa_j)^2}{(n_i + n_j)^2 + (\kappa_i + \kappa_j)^2} \right| \exp(i\theta_{ij}) \quad (4)$$

$$\times [ij=0,1,2,3, \quad r_{ij} = -r_{ji}, \quad \theta_{ij} = \arg(r_{ij})]$$

are, respectively, the Fresnel reflection coefficients of air/AlGaIn, AlGaIn/GaN, and GaN/sapphire, and the corresponding transmission coefficient $t_{ij} = 1 + r_{ij}$. α is the absorption coefficient, n the refractive index, and d the thickness; $\delta_1 = (4\pi/\lambda)n_1 d_1$ and $\delta_2 = (4\pi/\lambda)n_2 d_2$, $\kappa_1 = \alpha_1 \lambda / 4\pi$ and $\kappa_2 = \alpha_2 \lambda / 4\pi$.

Using Eqs. (3), the reflectance spectra of AlGaIn/GaN heterostructure was numerically calculated. In the calculation, the absorption coefficient spectrum of GaN was taken from our previous work;¹⁷ the absorption spectrum of AlGaIn was obtained from the rigid shift of GaN. For avoiding noticeable error, the Al mole fraction of AlGaIn is set to be a relatively low value, $x \leq 0.11$. The energy locations of the maxima of excitonic profiles in the absorption spectra of GaN and AlGaIn, named E_{GM} and E_{AM} , respectively, were used as identifications corresponding to the extreme in reflectance spectrum. Published data of Brunner *et al.* were used for the refractive index of GaN and $\text{Al}_{0.1}\text{Ga}_{0.9}\text{N}$ as a function of composition x and energy below the band gap.¹⁸ Above the band gap, the data of Amano *et al.* were employed.¹⁹ Sapphire is considered to be transparent with the refractive index as a function of wavelength quoted from Ref. 20. It should be mentioned that the phase factor $\exp(i\theta_{ij})$ in Eq. (4) may also contribute to the phase shift in reflectance spectrum. However, this is neglected in the most of the literature.

The details in the reflectance spectra can be explained by the calculated spectrum illustrated in Fig. 2. As expected, model calculations show that the excitonic structures in absorption spectra of GaN and AlGaIn are just the cause of the

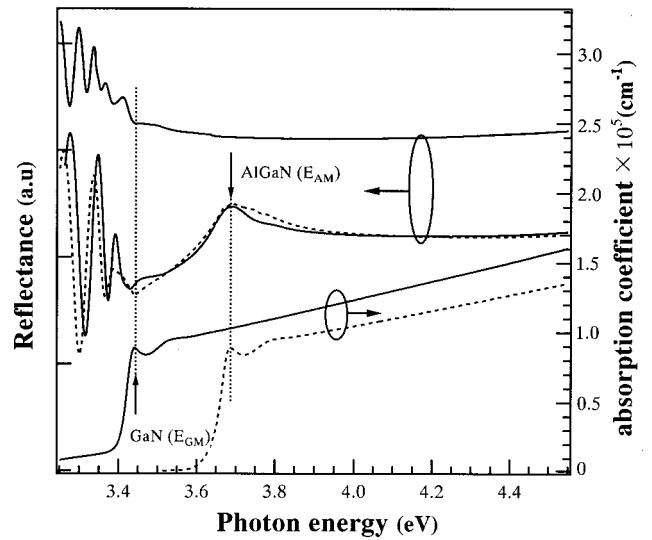


FIG. 2. Numerically calculated reflectance spectral of $\text{Al}_{0.11}\text{Ga}_{0.89}\text{N}/\text{GaN}/\text{sapphire}$ heterostructure (dashed line). The solid line represents the experimental data. Reflectance and absorption spectra of the GaN/sapphire structure are also given for comparison. E_{GM} and E_{AM} were used as identification responding to the maxima of exciton profiles in absorption spectra of GaN (solid line) and $\text{Al}_{0.11}\text{Ga}_{0.89}\text{N}$ (dashed line), respectively.

corresponding valley and peak in the reflectance spectrum. As shown in Fig. 2, the reflectance can be divided into three regions, which are the photon energy (a) below the absorption edge of GaN; (b) between the absorption edges of GaN and AlGaIn; and (c) above the absorption edge of AlGaIn.

In region (a), as the normal-incidence beam experiences relatively weak absorption, the reflected beam consists of the lights that reflected from the interfaces of air/AlGaIn, AlGaIn/GaN, and GaN/sapphire. In this region, the reflectance spectrum is dominated by the interference effect results from both AlGaIn and GaN layers phase factor $\exp(-j\delta_1)$ and $\exp(-j\delta_2)$. In region (b), due to the strong absorption of the GaN layer, the second term in Eq. (3) tends to be negligible, and results in a drastic change in reflectance. Since the multiple reflections in the GaN layer were eliminated in this region, the reflected beam only comes from the lights reflected at interfaces of air/AlGaIn and AlGaIn/GaN, and the shape of the reflectance spectrum is mainly dominated by the interference effect results from $\exp(-j\delta_1)$. As the energy of incident light further increases and reaches into region (c), the absorption of AlGaIn rapidly increases, resulting in a sharp change in reflectance again.

Besides the excitonic resonance structures of GaN and AlGaIn, we would like to address the line shape of reflectance spectrum region (b), where the interference effect caused by the AlGaIn layer may strongly modify the spectral line shape and confuse the recognition of the excitonic profile desired. Figure 3 displays the experimental reflectance spectra of different thicknesses of AlGaIn layers. For Al composition x around 0.1, we can see that the variation of d_1 result in noticeable changes in the spectral line shapes of region (b). Specially, we found that when d_1 is about 200 nm [Figs. 3(c) and 3(d)], the reflectance spectra show quite a difference in shape. In Fig. 3(c), ‘‘two peaks’’ appear near

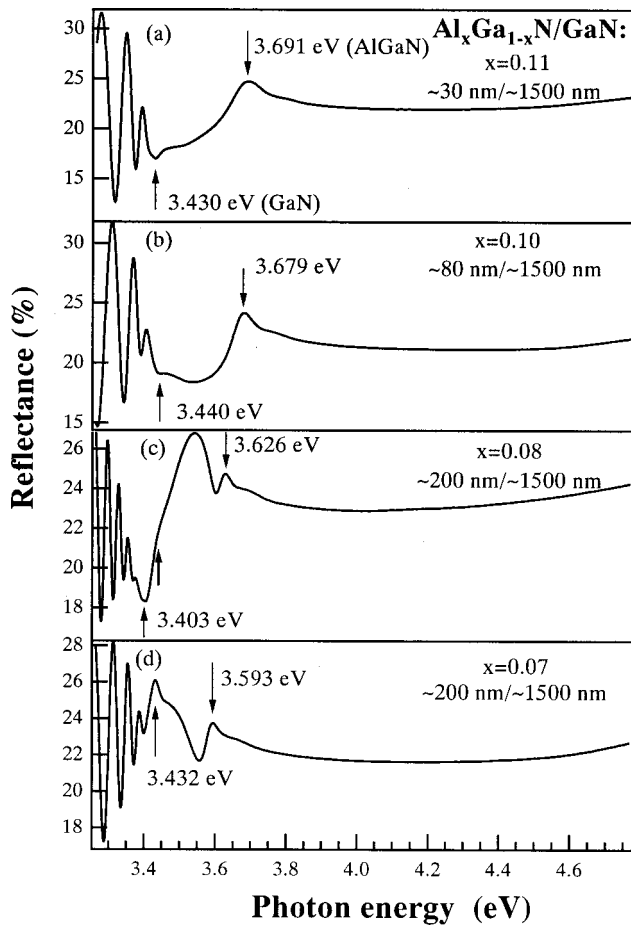


FIG. 3. Experimental reflectance spectra for $\text{Al}_x\text{Ga}_{1-x}\text{N}/\text{GaN}/\text{sapphire}$ (x around 0.1) heterostructures with various thicknesses of AlGaIn layers (d_1). The thickness values were measured by thickness monitor in the growth process of epilayers. It shows that the excitonic profile of GaN is hidden in interference fringes when d_1 is about 200 nm.

the excitonic position of AlGaIn and the excitonic profile of GaN seems to be hidden (3.403 eV seems to be an extremum value of interference fringes rather than a value of E_{GM} which is indicated by another arrow at about 3.43 eV); however, in Fig. 3(d) the excitonic peaks of GaN and AlGaIn can be identified clearly. In order to be clear in assigning both AlGaIn and GaN peaks from Figs. 3(c) and 3(d), the reflection model was again used to analyze the experimental spectra, where the thickness of the AlGaIn layer is a variable parameter. Because heterostructure devices are usually grown on thick GaN, where thickness enables the multiple reflection in the GaN layer diminished at energy above E_g^{GaN} , the influence of the variation in thickness of the GaN layer (d_2) was not found and, therefore, was not concerned here.

In Fig. 4, the calculated spectra of different thicknesses of AlGaIn layers are shown. As for the variation in thickness of the AlGaIn layer (d_1), it was seen that the energy location E_{AM} of the identification line does not shift with the changes of thickness d_1 , while the line shape changes just like the changes of the experimental one (Fig. 3). It was also found that the peak like shape presented below the E_{AM} [Fig. 4(c)] is a interference fringe result from the AlGaIn layer when d_1

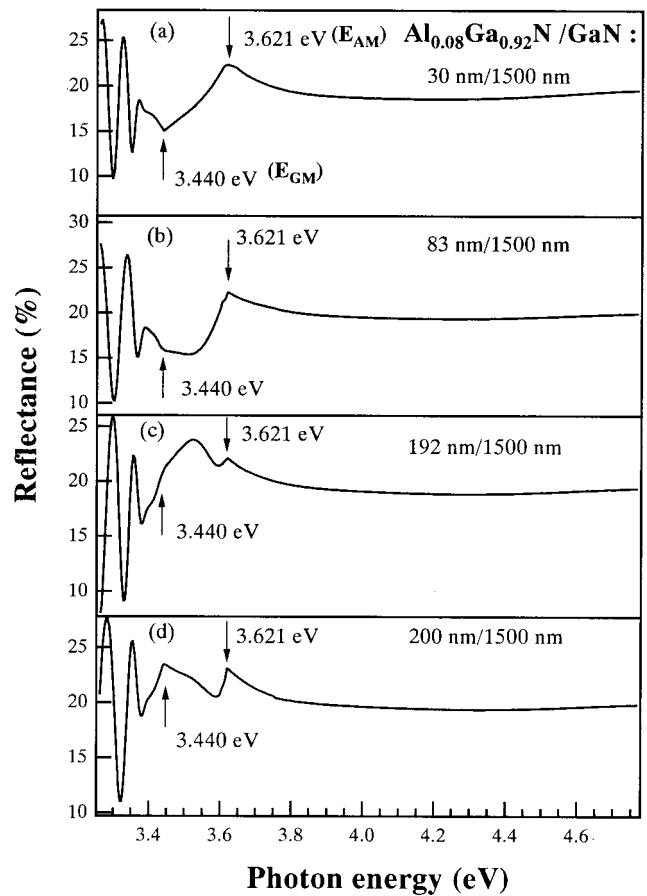


FIG. 4. Calculated reflectance spectra for $\text{Al}_{0.08}\text{Ga}_{0.92}\text{N}/\text{GaN}/\text{sapphire}$ heterostructures with thickness (d_1) changes corresponding to that in Fig. 3. The line shape of region (b) shows the changes in agreement with that in Fig. 3, while the energy location of E_{AM} (3.621 eV) are not shifted.

is 192 nm. Under the effect of this fringe, the excitonic profile of GaN is undistinguished, while that of AlGaIn is still visible. For interpretation, we utilized the calculated spectra of R_{01} ($R_{01} = |r_{01}|^2$) as shown in Fig. 5. It comes as no surprise that the line shape of R_{01} exhibits a trend to agree with that of R as the thickness d_1 increases. We can know that in regions (b) and (c), the large value of a_2d_2 of the GaN layer lets $R \approx R_{02}$ [see Eq. (3)]. According to Eq. (3a), r_{02} will approach r_{01} as the d_1 increases, meaning that thick enough d_1 will eliminate the multiple reflections in the AlGaIn layer and only leave the reflected light of r_{01} remaining. As a result, R will approach R_{01} . Figure 5 provides a direct observation that R_{01} acts as a dominant factor in the amplitude of power reflectance R around the exciton resonance energies of AlGaIn. Because R_{01} is not affected by the variation of thickness d_1 , the excitonic profile of AlGaIn cannot be diminished in the line shape changes. In contrast to the AlGaIn layer, the GaN layer has to reflect its excitonic profile through the reflected lights of r_{12} and r_{23} and, therefore, it is easily affected by the interference effect and its excitonic profile may be hidden by the interference fringe. The calculated model demonstrates that the occurrence of interference fringe starts from about $d_1 = 40$ nm with a thickness period about 75 nm.

We can summarize the results of the above analysis as

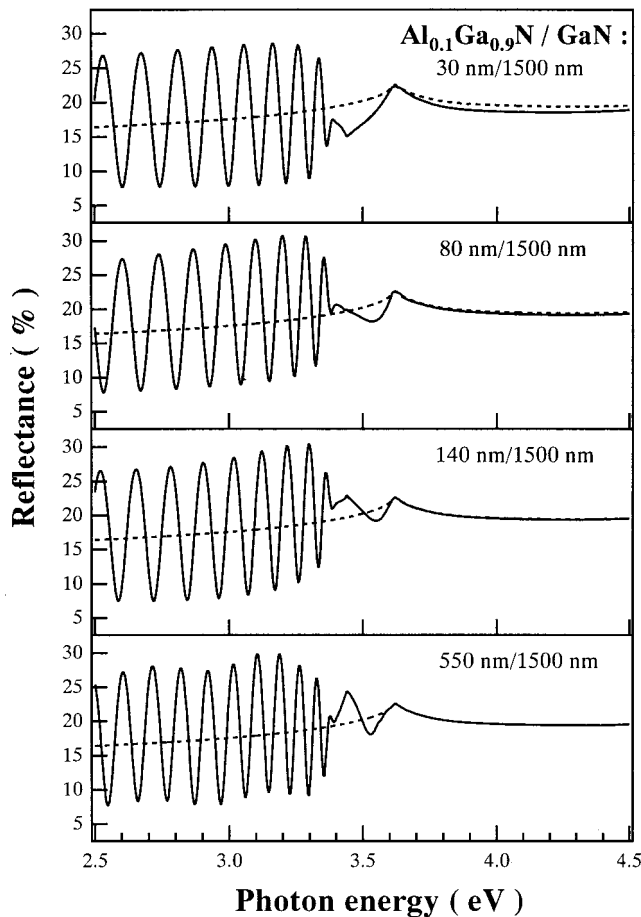


FIG. 5. Calculated reflectance spectra of R_{01} (dashed line) and R (solid line) with various thickness d_1 . With the increase of d , R_{01} shows a trend of agreement with R at the excitonic profile of AlGaN. It also shows the amplitude of R_{01} is a dominant part in that of R .

(i) without the presence of interference fringes [in region (b)], both excitonic profiles of GaN and AlGaN can be easily identified in the reflectance spectrum; (ii) with the presence of interference fringes, the excitonic profile of the GaN layer is possibly overlapped, but the excitonic profile of AlGaN can be observed. The interference fringes will only present at the low optical energy region of E_{FX} and not shift the excitonic position. This lets us easily assign the peak of AlGaN; (iii) the application of the reflectance measurement in AlGaN/GaN/sapphire heterostructures is not limited by the layer thickness of AlGaN (except the AlGaN layer is too thin to be detected).

Figure 6 illustrates the experimental reflection spectra of AlGaN (~30 nm)/GaN (~1500 nm) samples with various Al mole fractions as a function of the photon energy. The positions around peak and valley of the spectra were taken as the free excitonic transition energies (E_{FX}) of the AlGaN and GaN layers, respectively, as indicated by arrows. Determination of the location of E_{FX} will be described in the next section. At room temperature, the three characteristic excitons (A, B, and C) could not be individually observed and were arranged in one broadened valley. We can see that with the increase of Al composition x , the E_{FX} of AlGaN shows a clear shift to the high energy left. Another interest is that, for the samples of $x \leq 0.16$, the reflectance spectrum exhibits

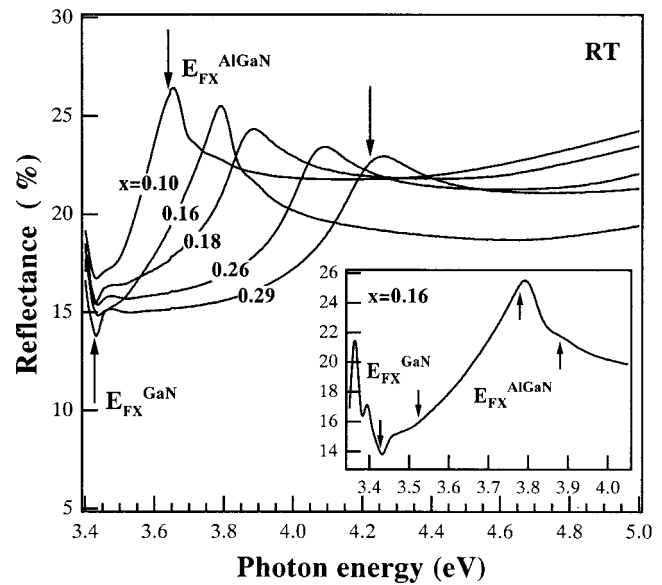


FIG. 6. Room temperature reflectance spectra of AlGaN (~30 nm)/GaN (~1500 nm) heterostructure samples with various Al mole fraction, x . The excitonic transition energies of GaN (E_{FX}^{GaN}) and AlGaN (E_{FX}^{AlGaN}) are marked by vertical arrows. The inset shows the spectrum of the $x=0.16$ sample. Broad features ascribed to exciton-LO phonon interaction were observed at optical energies about 100 meV above the E_{FX}^{GaN} and E_{FX}^{AlGaN} , respectively.

broad features at which the energy is about 100 meV above the free excitonic transition energies of GaN and AlGaN, respectively. Similar features have been reported by several studies in the absorption spectra of GaN epilayers taken at low²¹ and room temperature.²² However, to the best of our knowledge, there have been no reports on the observation of such features in neither absorption nor reflectance spectra of AlGaN alloys. It was suggested that this broad structure is due to the exciton-LO phonon interaction in an indirect phonon-assisted absorption process which an incident photon simultaneously generates a ground state free exciton and a LO phonon, resulting in a resonance feature at the corresponding energy in the spectrum. In the range of $0 \leq x \leq 0.15$, the LO-phonon energy of $Al_xGa_{1-x}N$ ranges from about 735 cm^{-1} (91.2 meV) to 770 cm^{-1} (95.5 meV).²³ By reason of the exciton dispersion, the energy spacing between the maximum of broad feature and the band edge exciton is slightly higher than one LO-phonon energy.²² The observed features indicate that LO phonon assisted exciton formation also plays an efficient part in the $Al_xGa_{1-x}N$ alloys (in this case, $x \leq 0.16$). For Al mole fraction above 0.16, the exciton-LO phonon interactions were no longer visible (Fig. 6) and may be attributed to the alloy broadening effect, due to the increase of Al content, which leads to a decrease of the Bohr radius of the free exciton in AlGaN²⁴ and makes the broad feature merge into the broadened excitonic profiles.

C. Free exciton transition energy and bowing parameter

In the spectral region which is of excitonic profile, we can determine the energy locations of the excitons with a

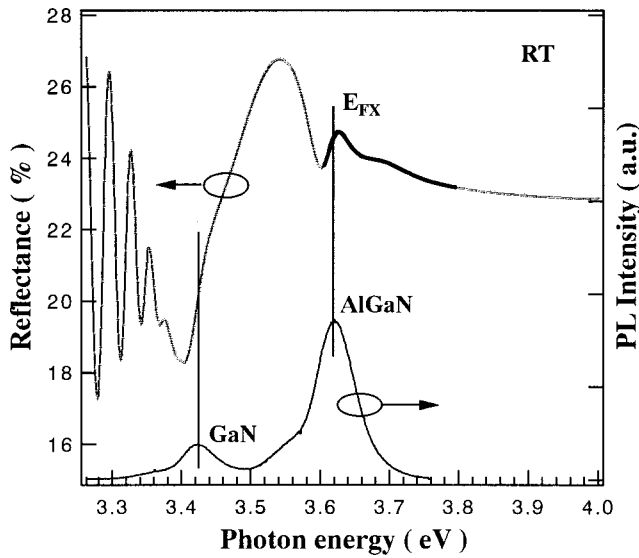


FIG. 7. A typical fitting curve of the experimental reflectance spectrum of the $\text{Al}_{0.08}\text{Ga}_{0.92}\text{N}/\text{GaN}$ heterostructure with the AlGaN layer about 200 nm. The free exciton transition energy (E_{FX}^A) obtained shows a good agreement with the peak energy of the PL spectrum.

simplified procedure. The spectral line shape due to the exciton transition of energy $h\nu_i$ can be approximately described in a form of Lorentzian dispersion,

$$R(\nu) = R_0 + A_i \text{Re} \left[\frac{h\nu_i - h\nu + i\Gamma_i}{(h\nu - h\nu_i)^2 + \Gamma_i^2} \exp(i\Theta_i) \right], \quad (5)$$

where R_0 is a constant of background reflectance, and A_i , $h\nu_i$, and Θ_i denote, respectively, the amplitude, the energy location, the broadening parameter, and the phase factor of exciton i ($i=A, B, C$).²⁵

At room temperature, the three discrete excitons (A , B , and C) could not be individually distinguished. However, they still have a strong impact upon the reflectance spectra that nonexcitonic models cannot fit.²⁶ In order to perform meaningful fits to the spectra, the minimum possible number of free parameters were tried. In the case of normal incidence, namely, $E \perp c$ axis, the resonance strength of the exciton C band to conduction band transition ($\Gamma_{1\nu}^7 \rightarrow \Gamma_c^7$) is very weak in the resonance length.²⁷ Therefore the exciton resonance structures in the reflectance spectra are dominated by the A and B exciton transitions here. Considering that the A and B excitons are relatively close in energy, we treated the A_i , Γ_i , and Θ_i of two excitons as the same one in the fitting process.

For the purpose of comparison, we also performed room temperature PL measurements on the samples of $x < 0.16$ AlGaN alloys, where the exciton resonance energies are below the excitation energy of the 325 He-Cd laser source (3.815 eV). A typical comparison of reflectance and PL spectra is shown in Fig. 7. The free exciton transition energy of A ($\Gamma_{1\nu}^9 \rightarrow \Gamma_c^7, E_{\text{FX}}^A$) is obtained by least-squares fit of Eq. (5) in reflectance spectrum. Table I summarizes the results of two measurements, and shows that the difference in E_{FX}^A of AlGaN is less than 6 meV. Such a result is acceptable because numerous studies have demonstrated the fact that for

TABLE I. Comparison of the free exciton transition energies (E_{FX}^A) of $\text{Al}_x\text{Ga}_{1-x}\text{N}$ ($x < 0.16$) epilayers determined from the reflectance spectra and the peak energies obtained from PL measurements.

Sample No.	1	2	3	4	5	6	7
PL E_g (eV)	3.533	3.578	3.600	3.621	3.667	3.669	3.695
Reflec. E_g (eV)	3.527	3.583	3.606	3.621	3.664	3.667	3.700

undoped GaN and its ternary compound AlGaN, the dominant peak in room temperature PL spectrum is due to the free exciton transition (FX).²⁸

Strictly speaking, the band gap energy is defined as the sum of free exciton transition energy (E_{FX}) and its binding energy (E_b), namely $E_g = E_{\text{FX}} + E_b$. However, the condition is complicated in the ternary compound AlGaN. Up to now the binding energy of AlN is not clear. Moreover, no precise knowledge is available on the composition dependence of effective masses in $\text{Al}_x\text{Ga}_{1-x}\text{N}$ ternary alloys so far. In practicality, the transition energy of free exciton can be treated as one of the most precise substitutes of true band gap energy (E_g), namely, the excitonic band gap.²⁹⁻³¹

The nonlinear dependence of the lowest direct band gap energy on the Al mole fraction can be written in the following expression:

$$E_g^{\text{AlGaN}} = E_g^{\text{GaN}}(1-x) + E_g^{\text{AlN}}x - bx(1-x), \quad (6)$$

where E_g (GaN) and E_g (AlN) are the room temperature band gap energies determined to be 3.43 and 6.20 eV for our samples.

The group values of x and E_g of AlGaN alloys were hence used to determine bowing parameter (b) by fitting Eq. (6). In Fig. 8, the fitting plot shows a value of $b=0.53$ eV, close to the reported value of 0.69 eV in Ref. 4 and 0.60 eV

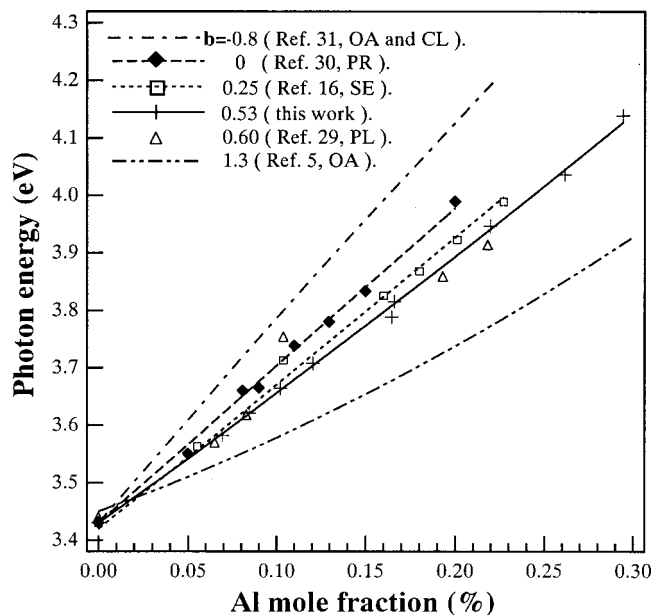


FIG. 8. Al composition dependence of the exciton transition energies derived from the reflectance measurement. Such dependencies of band gap energy derived from CL, OA, PL, PR, and spectroscopic ellipsometry (SE) methods in literature were shown together.

in Ref. 29. It is interesting to note that the samples used in Refs. 4 and 29 were close to the samples used here in structures. In addition, analysis of the measured c lattice parameter shows that the AlGaIn layers in all of the heterostructures were subjected to an in-plane tensile biaxial strain. It is known that the band gap, under the tensile strain, decreases relative to the unstained result. This in turn supports that the bowing in the AlGaIn band gap is downward.

IV. SUMMARY

In summary, a simple method combining the normal incident reflectance with XRD measurement to determine the Al mole fraction and bowing parameter of AlGaIn alloys was presented. By using a reflection model of two absorbing layers with a transparent substrate, the power reflectance of the AlGaIn/GaN/sapphire heterostructure was numerically calculated. The results of the model calculations show a good agreement with that of the experiments. Based on these calculations, a discussion concerning the confirmation of excitonic profile and the influence from the thickness variation of AlGaIn layer was performed. Analysis shows that the reflectance measurement is indeed feasible in determining the free exciton transition energy (E_{FX}) of the AlGaIn epilayer in the AlGaIn/GaN heterostructure.

A precise value of E_{FX} was obtained by performing theoretical fit on the excitonic profile of a AlGaIn epilayer. Comparing with He–Cd laser source PL measurement, it was found that the difference between the E_{FX}^A and the corresponding peak energy is less than 6 meV. In the low Al composition ($x \leq 0.16$), the reflectance spectral features of exciton-LO phonon interaction were observed at an optical energy ~ 100 meV above the transition energy of band edge exciton of AlGaIn. This observation indicates that the samples under investigation are of high quality and also provides support that the energy locations of E_{FX}^A identified are correct. With consideration of in-plane biaxial strain, Al mole fractions were determined by using both lattice parameters of a and c obtained from XRD measurement by using the Bond method. In the composition range of $0 \leq x < 0.3$, we found a downward bowing in the band gap of the AlGaIn epilayer with a bowing parameter of $b = 0.53$.

The authors would like to thank Dr. Arulkumaran for his help and useful discussions. This work was supported, in part, by a Grant-in-Aid for Scientific Research(C) (Grant No. 09650049) from the Ministry of Education, Science, Sports, and Culture, Japan.

- ¹M. A. Khan, A. Bhattarai, J. N. Kuznia, and D. T. Olson, *Appl. Phys. Lett.* **63**, 1214 (1993); M. A. Khan, M. S. Shur, J. N. Kuznia, Q. Chen, J. Burn, and W. Schaff, *ibid.* **66**, 1083 (1995); S. N. Mohammad, Z. F. Fan, A. Salvador, O. Aktas, A. E. Botchkarev, W. Keim, and H. Morkoc, *ibid.* **69**, 1420 (1996); Q. Chen, M. A. Khan, J. W. Yang, C. J. Sun, M. S. Shur, and H. Park, *ibid.* **69**, 794 (1996).
- ²S. Itoh *et al.*, *Jpn. J. Appl. Phys., Part 2* **32**, L1530 (1993); R. L. Aggarwal, P. A. Maki, R. J. Molnar, Z. L. Liao, and I. Melngailis, *J. Appl. Phys.* **79**, 2148 (1996).
- ³G. Y. Xu, A. Salvador, W. Kim, Z. Fan, C. Lu, H. Tang, H. Morkoc, G. Smith, M. Estes, B. Goldenberg, W. Yang, and S. Krishnankutty, *Appl. Phys. Lett.* **71**, 2154 (1997).

- ⁴S. R. Lee, A. F. Wright, M. H. Crawford, G. A. Petersen, J. Han, and R. M. Biefeld, *Appl. Phys. Lett.* **74**, 3344 (1999), and references therein.
- ⁵H. Angerer, D. Brunner, F. Freudenberg, O. Ambacher, M. Stutzmann, R. Hopler, T. Metzger, E. Born, G. Dollinger, A. Bergmaier, S. Karsch, and H.-J. Korner, *Appl. Phys. Lett.* **71**, 1504 (1997).
- ⁶H. Ehrenreich, H. R. Philipp, and J. C. Phillips, *Phys. Rev. Lett.* **8**, 59 (1962); H. R. Philipp and J. Ehrenreich, *Phys. Rev.* **129**, 1550 (1963).
- ⁷D. D. Sell, *Phys. Rev. B* **6**, 3750 (1972); D. D. Sell, H. C. Casey, Jr., and K. W. Wecht, *J. Appl. Phys.* **45**, 2650 (1974).
- ⁸W. Shan, B. D. Little, A. J. Fischer, J. J. Song, B. Goldenberg, W. G. Perry, M. D. Bremser, and R. F. Davis, *Phys. Rev. B* **54**, 16369 (1996); R. Stepniewski, K. P. Korona, A. Wyszomolka, J. M. Baranowski, K. Pakula, M. Potemski, G. Martinez, I. Grzegory, and S. Porowski, *ibid.* **56**, 15151 (1997).
- ⁹T. J. Ochalcki, B. Gil, P. Lefebvre, N. Grandjean, J. Massies, and M. Leroux, *Solid State Commun.* **109**, 567 (1999); T. J. Ochalcki, B. Gil, P. Lefebvre, N. Grandjean, J. Massies, M. Leroux, S. Nakamura, and H. Morkoc, *Appl. Phys. Lett.* **75**, 1419 (1999).
- ¹⁰L. S. Yu, D. Qiao, S. S. Lau, and J. N. Redwing, *Appl. Phys. Lett.* **75**, 1419 (1999).
- ¹¹T. Detchprohm, K. Hiramatsu, K. Itoh, and I. Akasaki, *Jpn. J. Appl. Phys., Part 2* **31**, L1454 (1992).
- ¹²F. A. Ponce, J. S. Major, Jr., W. E. Plano, and D. F. Welch, *Appl. Phys. Lett.* **65**, 2302 (1994).
- ¹³M. Leszczynski, H. Teisseyre, T. Suski, I. Grzegory, M. Bockowski, J. Jun, S. Porowski, K. Pakula, J. M. Baranowski, C. T. Foxon, and T. S. Cheng, *Appl. Phys. Lett.* **69**, 73 (1996).
- ¹⁴M. Yamaguchi, T. Yagi, T. Azuhata, T. Sota, K. Suzuki, S. Chichibu, and S. Nakamura, *J. Phys.: Condens. Matter* **9**, 241 (1997).
- ¹⁵K. Tsubouchi and N. Mikoshiba, *IEEE Trans. Sonics Ultrason.* **SU-32**, 634 (1985).
- ¹⁶I. Akasaki and H. Amano, *Jpn. J. Appl. Phys., Part 1* **36**, 5393 (1997).
- ¹⁷G. Y. Zhao, H. Ishikawa, H. Jiang, T. Egawa, T. Jimbo, and M. Umeno, *Jpn. J. Appl. Phys., Part 2* **38**, L993 (1999).
- ¹⁸D. Brunner, H. Angerer, E. Bustarret, F. Freudenberg, R. Hopler, R. Dimitrov, O. Ambacher, and M. Stutzmann, *J. Appl. Phys.* **82**, 5090 (1997).
- ¹⁹H. Amano, N. Watanabe, M. Koide, and I. Akasaki, *Jpn. J. Appl. Phys., Part 2* **32**, L1000 (1993).
- ²⁰*Handbook of Optical Constants of Solids II*, edited by E. D. Palik (Academic, New York, 1991).
- ²¹J. F. Muth, J. H. Lee, I. K. Shmagin, R. M. Kolbas, H. C. Casey, Jr., B. P. Keller, U. K. Mishra, and S. P. DenBaars, *Appl. Phys. Lett.* **71**, 2572 (1997).
- ²²W. Shan, A. J. Fischer, S. J. Hwang, B. D. Little, R. J. Hauenstein, X. C. Xie, J. J. Song, D. S. Kim, B. Goldenberg, R. Horning, S. Krishnankutty, W. G. Perry, M. D. Bremser, and R. F. Davis, *J. Appl. Phys.* **83**, 455 (1998).
- ²³D. Behr, R. Niebuhr, J. Wagner, K.-H. Bachem, and U. Kaufmann, *Appl. Phys. Lett.* **70**, 363 (1997).
- ²⁴G. Steude, B. K. Meyer, A. Goldenr, A. Hoffmann, F. Bertram, J. Christen, H. Amano, and I. Akasaki, *Appl. Phys. Lett.* **74**, 2456 (1999).
- ²⁵K. P. Korona, A. Wyszomolka, K. Pakula, R. Stepniewski, J. M. Baranowski, I. Grzegory, B. Lucznik, M. Wrblewski, and S. Porowski, *Appl. Phys. Lett.* **69**, 788 (1996).
- ²⁶J. F. Muth, J. D. Brown, M. A. L. Johnson, Z. H. Yu, R. M. Kolbas, J. W. Cook, Jr., and J. F. Schetzina, *MRS Internet J. Nitride Semicond. Res.* **4S1**, G5.2 (1999).
- ²⁷R. Dingle, D. D. Sell, S. E. Stokowski, P. J. Dean, and R. B. Zetterstrom, *Phys. Rev. B* **3**, 497 (1971).
- ²⁸G. Steude, D. M. Hofmann, B. K. Meyer, H. Amano, and I. Akasaki, *Phys. Status Solidi A* **165**, R3 (1998); B. Monemar, J. P. Bergman, I. A. Buyanova, W. Li, H. Amano, and I. Akasaki, *MRS Internet J. Nitride Semicond. Res.* **1**, 2 (1996); S. Chichibu, T. Azuhata, T. Sota, and S. Nakamura, *J. Appl. Phys.* **79**, 2784 (1996).
- ²⁹G. Steude, D. M. Hofmann, B. K. Meyer, H. Amano, and I. Akasaki, *Phys. Status Solidi B* **205**, R7 (1998).
- ³⁰T. J. Ochalcki, B. Gil, P. Lefebvre, N. Grandjean, M. Leroux, J. Massies, S. Nakamura, and H. Morkoc, *Appl. Phys. Lett.* **74**, 3353 (1996).
- ³¹S. Yoshida, S. Misawa, and S. Gonda, *J. Appl. Phys.* **53**, 6844 (1982).